Energy and Buildings 133 (2016) 37–45

Contents lists available at ScienceDirect

Energy and Buildings

journal homepage: www.elsevier.com/locate/enbuild

A decision tree based data-driven diagnostic strategy for air handling units

Rui Yan [a], Zhenjun Ma [a,*], Yang Zhao [b], Georgios Kokogiannakis [a]

[a] Sustainable Buildings Research Centre (SBRC), University of Wollongong, NSW, 2522, Australia
[b] Institute of Refrigeration and Cryogenics, Zhejiang University, China

ARTICLE INFO

Article history:
Received 11 May 2016
Received in revised form 10 August 2016
Accepted 20 September 2016
Available online 21 September 2016

Keywords:
Decision tree
CART
Feature selection
Air handling unit
Fault diagnosis
Interpretability

ABSTRACT

Data-driven methods for fault detection and diagnosis of air handling units (AHUs) have attracted wide attention as they do not require high-level expert knowledge of the system of concern. This paper presents a decision tree based data-driven diagnostic strategy for AHUs, in which classification and regression tree (CART) algorithm is used for decision tree induction. A great advantage of the decision tree is that it can be understood and interpreted and therefore its reliability in fault diagnosis can be validated by both testing data and expert knowledge. A steady-state detector and a regression model are incorporated into the strategy to increase the interpretability of the diagnostic strategy developed. The proposed strategy is validated using the data from ASHRAE 1312-RP. It is shown that this strategy can achieve a good diagnostic performance with an average F-measure of 0.97. The interpretation of the diagnostic decision tree using expert knowledge showed that some diagnostic rules generated in the decision tree comply with expert knowledge. Nevertheless, the interpretation also indicated that some diagnostic rules generated are not reliable and some of them are only valid under certain operating conditions, which indirectly demonstrated the importance of the interpretability of fault diagnostic models developed using data-driven methods.

1. Introduction

The operation of building Heating, Ventilation, and Air-Conditioning (HVAC) systems is vulnerable to various faults, and the occurrence of any fault could lead to increased energy consumption or indoor thermal discomfort [1,2]. Successful detection and isolation of any faults in HVAC systems in a timely manner can improve building energy efficiency and reduce carbon footprint.

Over the last two decades, considerable efforts have been made in the development of fault detection and diagnosis (FDD) strategies for building HVAC systems [3–5]. Fault detection is a process that determines whether or not an HVAC system is operating in a healthy condition while fault diagnosis aims to identify the causes of the fault. Compared to fault detection, fault diagnosis is more challenging and complicated. The existing FDD methods can be generally categorised into model-based methods, rule-based methods and data-driven methods [6]. Data-driven methods have attracted wide attention as they do not require high-level expert knowledge of the system and the computational costs are generally manageable [4].

Air handling unit (AHU) is one of the important components in HVAC systems and a number of studies have been focused on detection and diagnosis of various faults in AHUs. For instance, a rule-based FDD strategy for AHU temperature sensors was developed by Yang et al. [7], in which a set of if-then rules were formulated based on expert knowledge. The performance evaluation using the data from a green building and a small scale AHU simulator showed that this strategy is capable of isolating AHU sensor faults under different operating modes. A FDD strategy based on Bayesian Belief Network (BBN) for AHUs was presented by Zhao et al. [8,9], in which a probabilistic graphical model was used to represent the relationships of probabilistic dependencies within different variables. It was shown that this method can successfully isolate common faults occurred in AHUs. A drawback of this method is that it requires high-level expert knowledge, especially in determining the probability parameters. A sensor fault detection strategy for AHUs using cluster analysis was developed by Yan et al. [5], in which the clustering algorithm Ordering Points to Identify the Clustering Structure (OPTICS) was used to identify the spatial separated data groups which possibly indicate the occurrence of sensor faults. Wang et al. [10] described a hybrid FDD method

* Corresponding author.
E-mail addresses: mzjxjtu@163.com, zhenjun@uow.edu.au (Z. Ma).

http://dx.doi.org/10.1016/j.enbuild.2016.09.039
0378-7788/

Nomenclature

Symbols

a_1-a_3	Coefficients
α	Complexity parameter
c	Total number of class
F	Air flow rate (m^3/min)
FN	False negative
FP	False positive
I	Impurity measure
N	Fan speed control signal (%)
n	Number of observations
P	Power (W) or the proportion of the observations
p	Probability of the observations in a node
R	Misclassification rate
r	Node misclassification rate
s	Split
T	Temperature (°C)
t	Node for splitting
TP	True positive
U	Valve control signal (%)

Subscripts

cc	Cooling coil
L	Left
ma	Mixed air
oa	Outdoor air
R	Right
rf	Return fan
sa	Supply air
sf	Supply fan

which combines physical models and expert rules for variable air volume AHUs. To increase the model accuracy, genetic algorithms were used to determine the parameters of the model.

Data-driven based fault diagnosis methods were primarily developed based on pattern classification techniques [11]. The data-driven FDD methods for AHUs can be generally categorised into statistic based methods [12–14] and machine learning based methods [6,15–17]. Principal Component Analysis (PCA) and Fisher Discriminant Analysis (FDA) are two common statistic based methods. PCA is a multivariate analysis method which transforms the data set into a new set of uncorrelated variables so that the first few principal components retain the most of the variations [18]. Wang and Xiao [12], for example, presented a PCA-based AHU sensor FDD method, in which AHU sensor faults were detected by comparing the PCA model prediction error with a pre-defined threshold while fault diagnosis was achieved by using Q-contribution plot. It was shown that PCA is capable of extracting major information from the data with high dimensions and then presenting it in lower dimensions. FDA is a classifier based on linear dimensionality reduction techniques and is optimal in terms of maximising the separations among different classes. Du and Jin [14] used PCA for fault detection and FDA for fault diagnosis of AHU sensor faults. In a two-step AHU sensor fault detection and isolation strategy developed by Padilla and Choinière [19], PCA was used in the first step for fault detection while active functional testing was used in the second step for fault isolation. Among the machine learning-based methods, the use of artificial neural networks (ANNs) for AHU FDD has been extensively studied [6,20–24]. An ANN-based AHU FDD strategy was developed by Lee et al. [22]. Seven user-defined residual variables between the predicted and measured values were fed into a two-layer feed-forward ANN trained by back-propagation with both normal and faulty data. Eight typical AHU sensor and mechanical faults were considered. The results showed that this ANN-based FDD method can identify the root cause of AHU faults. An AHU FDD strategy using ANN and wavelet analysis was developed by Fan et al. [20]. Back-propagation neural network (BPNN) was used for AHU fault detection while Elman neural network coupled with wavelet analysis was used for fault diagnosis. Support vector machine (SVM) is another commonly used machine learning method for AHU FDD. Liang and Du [16] proposed a diagnostic strategy for AHUs based on support vector machine (SVM) method. This strategy can isolate different fault classes through finding the boundary that can maximize the margins between the classes. Four physical models were formulated and the residuals between the predicted and actual values were used as the input variables of the SVM classifier. It was found that the diagnostic accuracy of the SVM-based method mainly relies on the selection of the SVM kernel function. Mulumba et al. [17] described a model-based FDD strategy with SVM classification and an autoregressive model with exogenous variables (ARX) for AHU FDD. The supply air humidity was selected as a dependent variable while the supply air temperature and mixed air temperature were selected as the exogenous variables for the ARX model using ReliefF-based feature selection. The performance of the SVM-based method was compared with the classifiers such as ANN, random forest, and Naïve Bayes. It was shown that the SVM-based method outperformed the other methods in terms of the diagnostic accuracy. Wall et al. [25] described an AHU FDD method using a dynamic Bayesian network (DBN). DBN is similar to BBN but with an extra dimension of time. In contrast to the BBN-based method proposed in [8] in which the BBN parameters were estimated by expert knowledge, the parameters in DBN were obtained using both normal and faulty training data.

Although data-driven FDD methods are promising when validated using the testing data, a key drawback of this approach is that most data-driven methods (e.g. ANN and SVM-based) were developed based on black-box models, which means that it is almost impossible to understand how faults are isolated. As the actual fault diagnostic accuracy of data-driven methods heavily relies on the quality of training data used, the factors such as lacking of unique data patterns and errors in the training data may result in invalid classification. In many cases, only a limited amount of training data is available, which usually cannot cover the full operation range of the system of concern. The model developed may therefore only valid under certain operating conditions. Without interpretability, it is difficult to know whether or not the model used is reliable and under what operating conditions the model is reliable.

This paper presents a decision tree based data-driven method for fault diagnosis of AHUs. Decision tree, as a well-known classifier, has been applied in prediction of building energy usage with satisfied accuracy [26,27]. Compared to other data-driven diagnostic strategies, the proposed strategy is interpretable by using the decision tree which can generate a set of if-then rules. The interpretability of the proposed strategy can be helpful in understanding the diagnostic strategy for isolating different AHU faults. The proposed strategy can also automatically perform feature selection, which often requires considerable efforts to analyze and define the key features in data-driven FDD strategies [28].

2. Outline of the diagnostic strategy

The outline of the proposed AHU diagnostic strategy is illustrated in Fig. 1. The overall strategy consists of three steps including 1) data preparation; 2) decision tree induction and evaluation and; 3) decision tree interpretation.

The fault-free data is first used to determine the coefficients of a regression model, as shown in Eq. (1) [8]. This regression model is used to generate a residual feature in order to reduce the

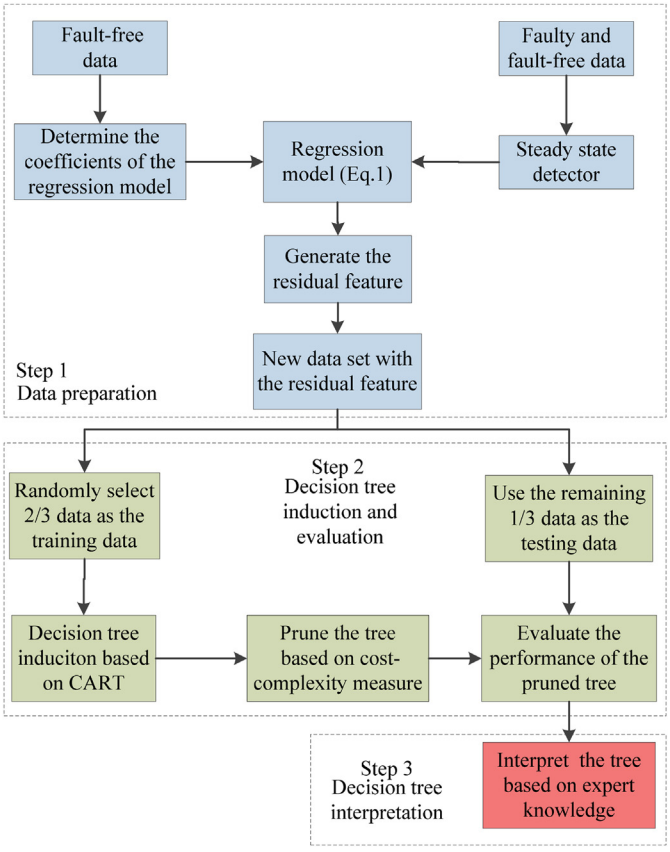

Fig. 1. Outline of the proposed AHU fault diagnostic strategy.

complexity of the decision tree to be developed. The recorded fault-free data and the data labelled with different AHU faults are then processed using a steady state detector to filter out the data in the transient period in order to improve the accuracy of fault diagnosis and reduce the complexity of the decision tree. The details of the steady state detector used are the same as that used in [8,29]. Using the regression model and the filtered data, the residual between the measured and predicted fan speed control signal can be generated and a new data set with this new feature (i.e. residual) and all filtered data can be prepared for fault diagnosis.

$$N_{sf} = a_1 F_{sa}^2 + a_2 F_{sa} + a_3 \tag{1}$$

where F_{sa} and N_{sf} are the supply air flow rate and supply fan speed control signal respectively, and a_1-a_3 are the coefficients.

The second step, i.e. decision tree induction and evaluation, is the core of the diagnostic strategy. Firstly, 2/3 of the data in the new data set is randomly selected and used as the training data for decision tree induction based on the classification and regression tree (CART) algorithm, which will be elaborated in Section 3. The decision tree is initially fully grown in order to capture all possible diagnostic rules. However, a fully grown tree usually has too many branches which make the model interpretation difficult and may result in over-fitting. It is, therefore, necessary to prune the tree by using appropriate methods. In CART, the cost-complexity measure is used for tree pruning purpose. After the decision tree is pruned, the rest data in the prepared new data set is then used to test and validate the accuracy of the diagnostic decision tree developed based on the F-measure defined in Eq. (2). The F-measure is a commonly used binary classification accuracy measure [30].

$$\text{F-measure} = \frac{2 \times TP}{2 \times TP + FP + FN} \tag{2}$$

where *TP* is the true positive, *FP* is the false positive and *FN* is the false negative. Positive denotes the data with the targeted labels while negative denotes the data with all other labels.

The last step is the interpretation of the post-pruned decision tree by using expert knowledge in order to confirm whether the diagnostic rules generated are valid and have physical meanings.

3. Decision tree induction

CART is a widely used decision tree induction method, in which the decision tree is constructed by recursively partitioning the data space and fitting a prediction model within each partition [31]. The partitions are graphically represented as a binary decision tree. Unlike other commonly used tree induction methods such as C4.5 and Chi-square Automatic Interaction Detector (CHAID) which can be used for classification only, CART can be used for both classification and regression [32]. In this study, CART is used as a classification tree induction method for constructing the diagnostic model.

For the classification tree induction, CART evaluates the split point based on the goodness of the split criteria as shown in Eq. (3) [33], where the impurity measure *I* used in CART is the *Gini* impurity measure as defined in Eq. (4) [30]. The best split is at the point where $\Delta \mathrm{I}(s, t)$ is maximised. As *I(t)* is a fixed value for a given point, maximising the goodness of the fit is equivalent to minimising the weighted average impurity measure of the child nodes [30]. If there are no stopping criteria provided, the tree will continuously grow until all observations in the node have the same class or the number of the observations in the node is below a predefined threshold.

$$\Delta \mathrm{I}(s, t) = I(t) - (P_L(I(t_L)) + P_R(I(t_R))) \tag{3}$$

$$\mathrm{Gini}(t) = 1 - \sum_{i=0}^{c-1} [p(i|t)]^2 \tag{4}$$

where $\Delta \mathrm{I}(s, t)$ stands for the impurity difference before and after a split, s stands for a particular split, t is the node for splitting, t_L and t_R are the left and right child nodes of t respectively, P_L and P_R denote the proportions of the observations at node t that go into the left and right child nodes respectively, $p(i|t)$ stands for the fraction of the observations in class i at a given node t, and c is the total number of classes.

As mentioned before, a fully grown classification tree could have two disadvantages. The first is the over-fitting problem, which means that the model performs extremely well with the training data but performs poorly with the testing data [30]. The second disadvantage is that a fully grown classification tree is difficult to be understood and interpreted. CART provides a cost-complexity based tree pruning strategy, which can optimize the trade-off between the cost of misclassification and the tree complexity. The cost from the number of leaf nodes is measured by a non-negative complexity parameter α as defined in Eq. (5) [34].

$$\alpha = \frac{R(t) - R(T)}{|\tilde{T}| - 1} \tag{5}$$

where $\tilde{T}$ is the leaf nodes of the subtree T, $|\tilde{T}|$ is the number of the leaf nodes, *R(T)* is the tree misclassification rate defined in Eq. (6), and *R(t)* is a single node misclassification rate defined in Eq. (7), in which *r(t)* is defined in Eq. (8) [34].

$$R(T) = \sum\nolimits_{t \in \tilde{T}} R(t) \tag{6}$$

$$R(t) = r(t)\, p(t) \tag{7}$$

$$r(t) = 1 - max_i p(i|t) \tag{8}$$

where *p(t)* is the probability of the observations in the node t, and max_i refers to the class i that results in the largest *p(i|t)*.

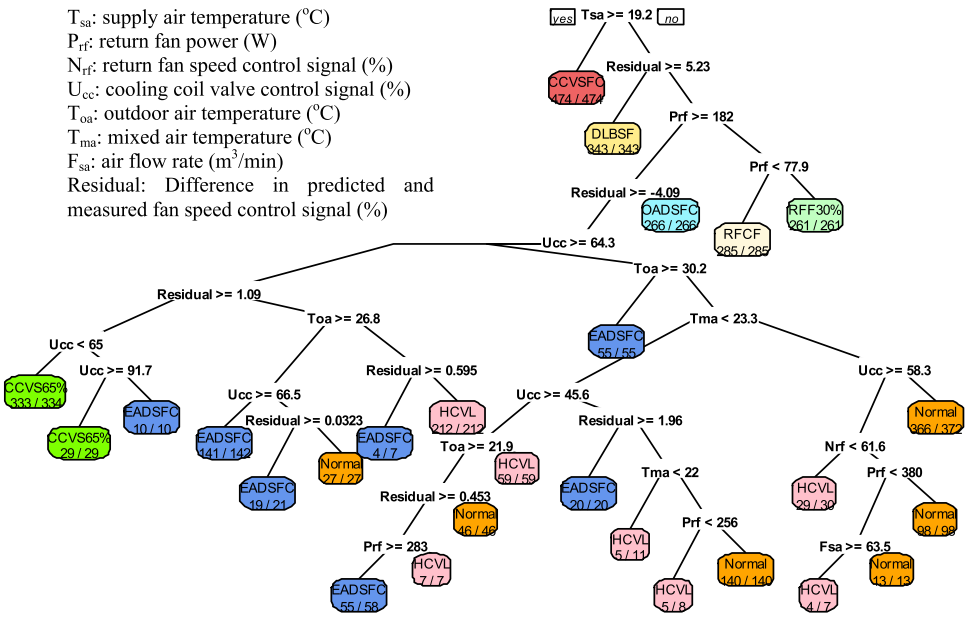

Fig. 2. The fully grown AHU fault diagnostic tree with the residual feature.

There are a finite number of α values corresponding to a sequence of pruned trees T_0, T_1,. . .,T_n. Each T_i in this sequence is characterised by a different value α_i. To generate the sequence, CART adopted an iterative algorithm starting with the fully grown tree (T_0) and the first pruned tree (T_1) is then developed by finding the node t ∈ T_0 that minimises Eq. (5) [35].

The minimum value of this function is the value of α_0 corresponding to T_0 and a new pruned tree T_1 is generated by pruning tree T_0 at the node t. The same procedure will be repeated based on tree T_1 and generates α_1 and T_2. The iteration terminates until the root node is reached.

Once the sequence of the minimal cost-complexity trees is generated, the final pruned tree can be determined by plotting the relative error (RE) versus the complexity parameters. The relative error of a decision tree is defined as in Eq. (9). The optimal prune point is the point where *RE* does not have any significant decrease if further decreasing the cost of complexity.

$$RE = 1 - \frac{n_{correct}}{n_{total}} \quad (9)$$

where $n_{correct}$ is the number of correctly classified observations and n_{total} is the total number of observations.

4. Validation and interpretation of the AHU diagnostic strategy

In this study, the proposed strategy was implemented in R [36] with CART implemented using the rpart [37] and rpart.plot [38] packages. The majority of figures presented were generated using R package ggplot2 [39].

4.1. Experimental data

The experimental data from ASHRAE project 1312-RP [40–42] was used to test and evaluate the proposed AHU fault diagnostic strategy. ASHRAE 1312-RP tested various AHU faults based on an experimental AHU facility. Each fault was tested for 12 h from 6.00a.m. to 6.00p.m. while the fault-free test was conducted for three days. The sampling rate was one minute. The details of the experimental AHU facility and how the faults were introduced and tested can be found in [41–43]. Table 1 summarizes the different AHU faults considered in this study. These faults are among the typical AHU mechanical faults and are commonly considered in AHU FDD studies.

The diagnostic strategy developed was validated based on the data collected under the AHU mechanical cooling mode tested during the summer period. In the mechanical cooling mode, the supply air temperature was controlled at 12.8 °C and the indoor temperature was maintained at 22.2 °C. The supply fan was controlled to maintain the supply air static pressure at 348 Pa while the return fan operating speed was maintained at 80% of the supply fan operating speed [40].

4.2. Classification tree induction

Based on the randomly selected 2/3 training data from the new data set, a fully grown decision tree with a minimum number of 20 observations in a leaf node was generated, as illustrated in Fig. 2. The total number of observations corresponding to each fault and fault free conditions used as the training data is presented in Table 1. The number of the observations in a leaf node is constrained in order to avoid generating a too large decision tree and also for making the visualization easier. The fully grown decision tree has a total of 26 splits. The root and internal nodes were labelled with the test conditions in order to split the observations with different characteristics while the leaf nodes were labelled with the classification results. The left branches of the root and internal nodes are the branches that met the node splitting criteria while the right branches did not. The number in the leaf node represents the number of the correctly classified observations out of the total number of the observations classified to this leaf node. For instance, 333/334 in the cooling coil valve stuck at 65% opening (i.e. CCVS65%) indicated that 333 observations were correctly classified to CCVS65% fault while one observation was mis-classified.

From Fig. 2, it can be seen that some faults such as cooling coil valve stuck at fully closed (i.e. CCVSFC) and AHU duct leakage before supply fan (i.e. DLBSF) can be easily isolated after only a few node splitting steps. However, isolating some faults such as the heating coil valve leakage (i.e HCVL) and exhaust air damper stuck at fully closed (i.e. EADSFC) required considerable partitions, which significantly decreased the interpretability of the diagnostic decision tree. Some leaf nodes only included a very small proportion of the

Table 1
Summary of AHU faults considered and their abbreviations.

Case No.	Fault description	Abbreviation	Number of data points used as training data
Fault 1	Heating coil valve leakage	HCVL	330
Fault 2	Cooling coil valve stuck at fully closed	CCVSFC	474
Fault 3	Cooling coil valve stuck at 65% opening	CCVS65%	364
Fault 4	Return fan fixed at 30% speed	RFF30%	261
Fault 5	Return fan completely failed	RFCF	285
Fault 6	Outdoor air damper stuck at fully closed	OADSFC	266
Fault 7	Exhaust air damper stuck at fully closed	EADSFC	313
Fault 8	AHU duct leakage before supply fan	DLBSF	343
Fault-free	Normal operation	/	699

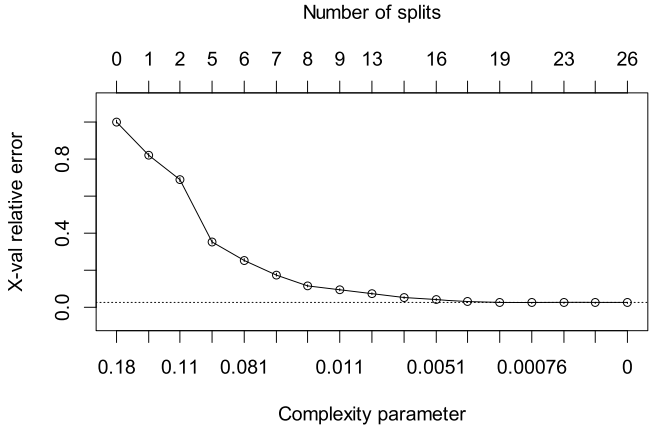

Fig. 3. Number of splits in the sequence of the pruned subtrees with different costs of complexity and the corresponding relative errors with the residual feature.

observations which indicated that the contributions from these branches to the diagnostic accuracy of the decision tree are not significant and can be generally neglected. Pruning these branches can result in a more interpretable classification tree while still remaining an acceptable diagnostic accuracy.

Fig. 3 illustrates the number of splits in the sequence of the pruned subtrees with different costs of complexity as well as the corresponding cross validated (X-val) relative errors. The X-val relative errors were calculated based on 10-folds cross validation. It should be noted that both horizontal axes are not in scale. The dashed line indicates the minimum relative error that can be achieved. More accurate values of the complexity parameters and their corresponding relative errors are summarized in Table 2. From Fig. 3 and Table 2, it can be seen that the cost of the complexity parameter between 0.00759 (i.e. corresponding the number of splits of 13) and 0.00531 (i.e corresponding number of splits of 14) is a good pruning point as the improvement of classification accuracy in terms of the relative error is insignificant if further decreasing the cost of the complexity parameter. The pruned decision tree with 14 splits is shown in Fig. 4. Compared to the fully grown tree, the overall fault diagnostic error was increased by 3.0% after the tree prune.

Table 2
Number of splits, corresponding complexity parameter and relative error.

Number of splits	Relative error	Complexity parameter
9	0.09219	0.01081
13	0.04895	0.00759
14	0.04135	0.00531
16	0.03073	0.00512
18	0.02049	0.00266
19	0.01783	0.00190
21	0.01404	0.00076
23	0.01252	0.00057
25	0.01138	0.00038
26	0.01100	0.00000

However, this relative error measure cannot reflect the impact of the tree pruning on the diagnostic accuracy of each individual fault.

To confirm whether the diagnostic accuracy is acceptable for individual faults, the performance of the pruned tree is evaluated in terms of F-measure using the testing data and the results are compared with that of the pre-pruned tree. The F-measures of the pre-pruned tree and post-pruned tree are summarized in Table 3. It can be seen that both pre-pruned and post-pruned diagnostic trees can completely isolate five faults including the cooling coil valve stuck at fully closed (Case 2), return fan fixed at 30% speed (Case 4), return fan completely failed (Case 5), outdoor air damper stuck at fully closed (Case 6) and AHU duct leakage before supply fan (Case 8), from the other faulty and fault-free cases. The F-measures of the other four cases considered were ranged from 0.94 to 0.99 for the pre-pruned decision tree and from 0.90 to 0.98 for the post-pruned decision tree. The largest decrease in the diagnostic accuracy was for the exhaust air damper stuck at fully closed (Case 7) and the corresponding F-measure was decreased from 0.96 for the pre-pruned tree to 0.90 for the post-pruned tree. The diagnostic accuracy of this fault is considered as acceptable in terms of the F-measure, as the symptom of this fault is very insignificant to be detected and isolated, as mentioned by Li and Wen [40].

The decision tree was also developed without including the residual feature in the new data set in order to demonstrate the necessity and importance of using this residual feature in the proposed strategy. Fig. 5 shows the number of splits in the sequence of the pruned subtrees with different costs of complexity as well as the corresponding relative errors. Compared to Fig. 3, the size of the decision tree is increased to 34 splits. Fig. 6 shows the post-pruned tree which was pruned at the point where the relative error is close to the relative error of the post-pruned decision tree with the residual feature. It is obvious that without considering the residual feature, the decision tree is hard to be interpreted due to the increased number of splits. Some faults such as AHU duct leakage before supply fan (i.e. DLBSF), and outdoor air damper stuck at fully closed (i.e. OADSFC), can be easily isolated by the decision tree generated with the residual feature. However, they required several splits to be successfully isolated without considering the residual feature.

Table 3
F-measures of different faults for pre-pruned and post-pruned diagnostic trees.

Case No.	Fault description	F-measure	
		Pre-pruned	Post-pruned
1	Heating coil valve leakage	0.94	0.90
2	Cooling coil valve stuck at fully closed	1.00	1.00
3	Cooling coil valve stuck at 65% opening	0.99	0.98
4	Return fan fixed at 30% speed	1.00	1.00
5	Return fan completely failed	1.00	1.00
6	Outdoor air damper stuck at fully closed	1.00	1.00
7	Exhaust air damper stuck at fully closed	0.96	0.90
8	AHU duct leakage before supply fan	1.00	1.00
9	Normal operation	0.97	0.93
	Average	0.98	0.97

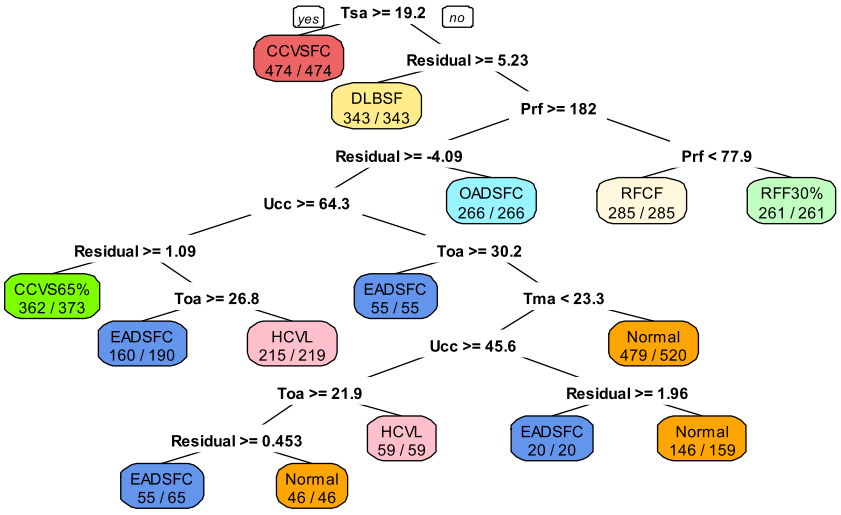

Fig. 4. Post-pruned AHU fault diagnostic tree with the residual feature.

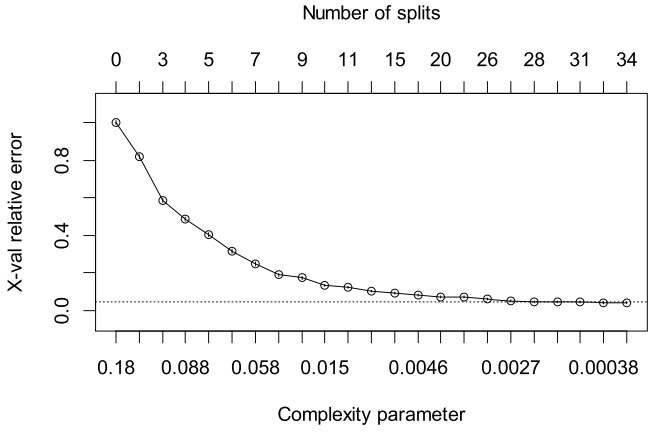

Fig. 5. Number of splits in the sequence of the pruned subtrees with different costs of complexity and the corresponding relative errors without using the residual feature.

4.3. Decision tree interpretation

In this section, the rules generated by the decision tree are interpreted in order to confirm the reliability of the proposed strategy. It is worthwhile to note that the following analysis is based on the faults investigated in this study (Table 1) without considering other possible AHU faults.

The five faults with F-measure of 1.0, which are also the top five branches of the diagnostic tree were first analyzed. The first split in Fig. 4 indicated that the AHU suffered from the cooling coil valve stuck at fully closed (i.e. CCVSFC) when the supply air temperature (T_{sa}) is not less than 19.2 °C. This rule is easy to understand as there is no chilled water supply when the cooling coil valve is fully stuck, and therefore the supply air cannot be cooled down to the required set-point.

The next split in Fig. 4 isolated the AHU duct leakage before supply fan (i.e. DLBSF) fault based on the residual between the predicted and actual supply fan speed control signal. If the difference between the predicted and the actual supply fan speed control signal is not less than 5.23%, the AHU will then be deemed as suffering

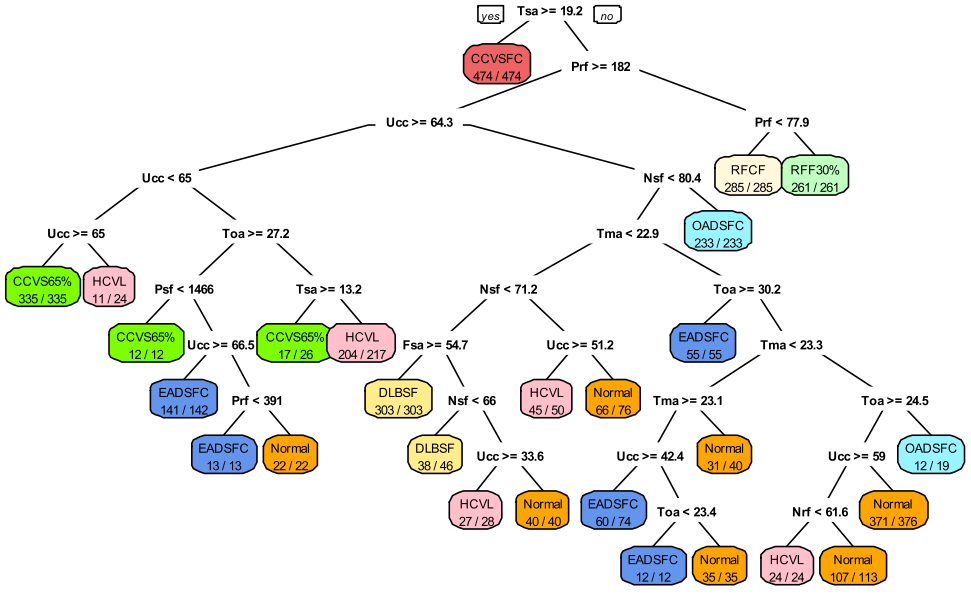

Fig. 6. Post-pruned AHU fault diagnostic tree without the residual feature.

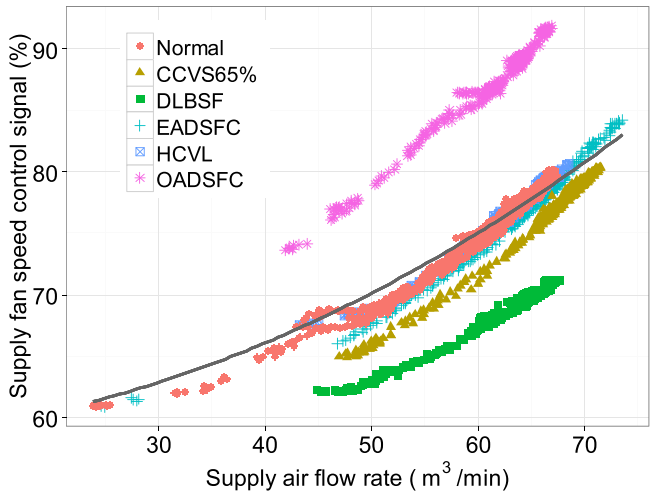

Fig. 7. Relationship between supply fan speed control signal and supply air flow rate under the faulty and fault-free conditions.

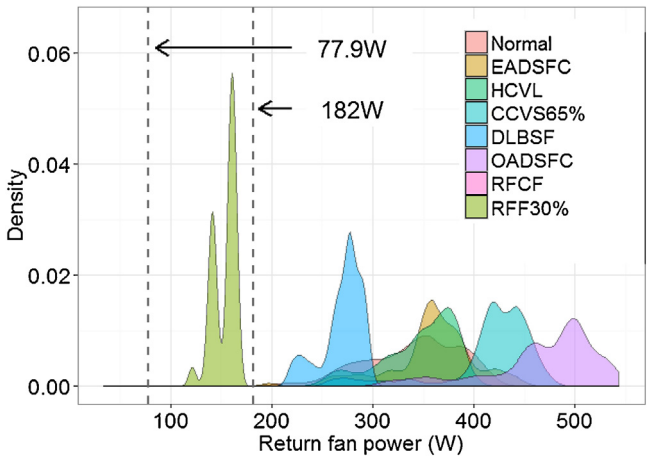

Fig. 8. Density distribution of the return fan power under the faulty and fault-free conditions.

from the DLBSF fault. This also complies with the expert knowledge that the duct leakage before the supply fan leads to a decreased duct resistance before the supply fan as the static pressure before the supply fan is negative. Fig. 7 illustrates the relationship between the AHU supply air flow rate and supply fan speed control signal under different faulty and fault-free conditions, where the black curve represents the predicted supply fan speed control signal under the fault-free conditions. A large deviation can be observed between the data points under the AHU normal operating condition and the operating condition suffering from the DLBSF fault, which clearly illustrates why the residual feature was selected by CART for isolating this fault. The patterns of other faults will be discussed later.

Once CCVSFC and DLBSF faults have been isolated, the return fan power was then selected as the next splitting feature. Fig. 8 shows the density distribution of the return fan power under the fault-free condition and all faulty conditions considered except the above two faults that have been isolated. It should be noticed that the density distribution of the return fan completely failed (i.e. RFCF) fault is not visible in Fig. 8 as the power of the return fan of all observations under the RFCF fault was 0. It is clearly shown that the boundary of the return fan power of 182 W can isolate the return fan fixed at 30% speed (RFF30%) and RFCF faults from the other faulty and fault-free conditions while the splitting point 77.9W was further picked up to separate the RFCF fault from the RFF30% fault. Actually, it is obvious that 77.9W is not the only point that can separate both faults as there is a large gap in the return fan power distribution under the RFCF fault and RFF30% fault conditions.

The residual feature was then further used to isolate the outdoor air damper stuck at fully closed (i.e. OADSFC) fault from the other non-isolated faulty and fault-free conditions. When the difference between the predicted and actual supply fan speed control signal is less than −4.09%, the CART determined that the outdoor air damper was stuck at fully closed. This is because that the fully closed outdoor air damper increased the duct resistance, resulting in a higher supply fan speed at a given air flow rate. This relationship can also be observed in Fig. 7.

After isolating all faults with F-measures of 1.0, further tree splitting isolated the following remaining faults, including the cooling coil valve stuck at 65% opening (i.e. CCVS65%) fault, exhaust air damper stuck at fully closed (i.e. EADSFC) fault and heating coil valve leakage (i.e. HCVL) fault, from the fault-free condition. The next split picked up the cooling coil valve control signal (*Ucc*) as the splitting feature, but without resulting in a leaf node. The left branch first isolated CCVS65% fault based on the residual feature. From Fig. 7, it can be seen that, for the remaining non-isolated faults, only the data of CCVS65% fault was not overlapped with the fault-free data, which indicated that CCVS65% fault may change the air duct resistance. However, this symptom did not match with the common knowledge that abnormal operation of the cooling coil valve should not result in a variation in the air duct resistance. ASHRAE 1312-RP report [40] mentioned that the control strategy of the test AHU facility opened the heating coil valve to maintain the supply air temperature if it is under the over-cooled condition. Nevertheless, the control strategy had a malfunction which led to fully close the outdoor air damper and exhaust air damper and fully open the return air damper. Due to the malfunction of the test AHU under CCVS65% condition, the training data of this fault was considered as invalid and was not representative to the AHU CCVS65% fault.

To isolate the exhaust air damper stuck at fully closed (i.e. EADSFC) and heating coil valve leakage (i.e. HCVL) faults, CART algorithm further selected the outdoor air temperature (T_{oa}) as a new splitting feature. If the outdoor air temperature is less than 26.8 °C, the AHU was more likely suffering from the HCVL fault. The isolation of faults based on the outdoor air temperature alone does not have any physical meaning, but could be meaningful when considered with the previous rule of the cooling coil valve opening (U_{cc}) that is not less than 64.3%. In another word, if the outdoor temperature is not very high but the cooling coil valve opening is relatively large, the AHU might experience the HCVL fault. This combined rule complies with the common knowledge that an HCVL fault will result in a larger cooling coil valve opening, which will be more significant under the low cooling load conditions. However, the cooling coil valve opening is not only influenced by the outdoor air temperature but also is influenced by the factors such as supply air flow rate, supply water temperature, etc. Therefore, a conclusive fault diagnostic result cannot be drawn based on these rules. Fig. 9 shows the isolated fault boundaries in terms of the cooling coil valve control signal and outdoor air temperature. The right bottom corner area with the light red color labelled as Condition 1 is the data space that the cooling coil valve opening (U_{cc}) is not less than 64.3% and the outdoor air temperature (T_{oa}) is less than 26.8 °C. As the majority data points in this region were with the heating coil valve leakage (i.e. HCVL) fault and some of them with the exhaust air damper stuck at fully closed (i.e. EADSFC) fault, it is therefore highly possible that the AHU is under the HCVL fault but this conclusion is not definite. Another leaf node labelled with the HCVL fault (see Fig. 4) was isolated in the same way, which labelled as Condition 2 in the area with the light brown color (Fig. 9). It deemed that the AHU is also under the HCVL fault if the cooling

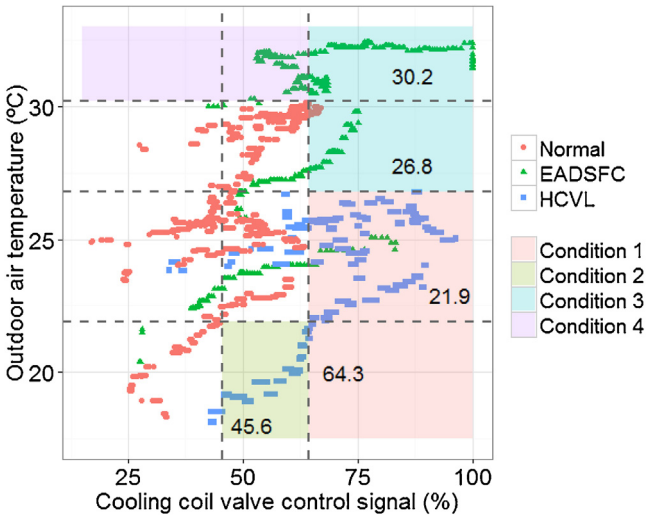

Fig. 9. Isolated fault boundaries in terms of the cooling coil valve control signal and outdoor air temperature.

coil valve opening is in the range of 45.6-64.3% and the outdoor air temperature (T_{oa}) is less than 21.9 °C.

If the outside air temperature is not less than 26.8 °C while the cooling coil valve opening (U_{cc}) is not less than 64.3%, it will be deemed that the AHU is suffering from the exhaust air damper stuck at fully closed (i.e. EADSFC) fault (see Fig. 4). These rules were also illustrated in Fig. 9 as Condition 3 labelled with the light blue. This diagnostic result might not be reliable as the maximum outdoor air temperature under the normal operating condition used as the training data is only 30.2 °C. Under the EADSFC fault condition, all return air will be re-supplied to the AHU and therefore a smaller cooling coil valve opening than that in the fault-free operation will be resulted in, under the mechanical cooling mode. The EADSFC fault was also isolated if the outdoor air temperature is not less than 30.2 °C and the cooling coil opening signal is less than 64.3% (Condition 4 in Fig. 9). This result may also not reliable due to the same reason as mentioned above.

The next split used the mixed air temperature (T_{ma}) as the splitting feature and isolated the normal condition from other faulty conditions. This is because that the fault-free case has more data points in this range than the other two faulty cases as shown in the histogram plot in Fig. 10. Splitting in this way can therefore

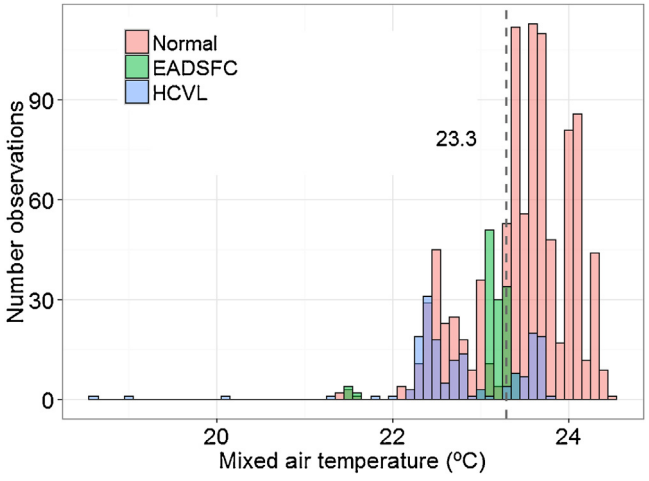

Fig. 10. Histogram plot of the number of the observations against different mixed air temperature.

minimize the impurity in the leaf nodes. However, these rules do not have a physical meaning. Furthermore, CART selected the residual feature to isolate the EADSFC fault from the normal operation as shown in Fig. 4. However, as illustrated in Fig. 7, the data pattern of the EADSFC fault is virtually completely overlapped by the data points in the normal operating conditions, and these two rules were therefore considered as unreliable.

In conclusion, the proposed CART-based AHU diagnostic strategy is able to easily isolate the AHU CCVSFC, DLBSF, RFCF, RFF30% and OADSFC faults. For the AHU HCVL fault, the proposed method cannot provide a conclusive diagnostic result, but the diagnostic outcome is highly valuable and can be used as a reference for further investigation. The proposed method is not able to successfully isolate the EADSFC fault as the symptom of this fault is insignificant.

The interpretation of the developed decision tree-based AHU diagnostic strategy demonstrated that, similar to many data-driven fault diagnostic strategies, the diagnostic accuracy and reliability of the proposed strategy rely on the information embedded in the training data. If the training data does not embody the unique data pattern of a particular fault, this fault is unlikely to be isolated, although the diagnostic accuracy of the strategy validated using the testing data may still be acceptable. The isolation of the CCVS65% fault showed that if the training data cannot reflect the actual operation of a specific fault, the developed diagnostic strategy can still isolate this fault if it is only validated by the randomly selected testing data. However, it might not be able to identify the target fault during the actual operation.

Therefore, the interpretability of a fault diagnostic strategy is essential to help understand how different faults are isolated. The proposed decision tree-based data-driven fault diagnostic strategy provides a meaningful way to develop an interpretable diagnostic strategy through generating a set of if-then rules in a binary tree form, which can help to validate the reliability of the developed diagnostic strategy.

5. Conclusion

This paper presented a data-driven AHU fault diagnostic strategy based on the Classification and Regression Tree (CART) method, which can automatically perform feature selection and therefore doesn't require considerable efforts to analyze and define the key features. Compared to black-box model based data-driven fault diagnostic strategies which do not have explicit physical meanings, the fault diagnostic results from the proposed strategy are interpretable. The interpretation of the developed diagnostic tree demonstrated that for most faults considered in this study, the fault diagnostic rules generated by the CART algorithm matched well with expert knowledge. It is also shown that the proposed CART-based fault diagnostic strategy can successfully identify relevant features to isolate different AHU faults. However, for some faults such as heating coil valve leakage and exhaust air damper stuck at fully closed, the rules generated were not valid or only valid under certain operating conditions, although a high diagnostic accuracy of the proposed strategy validated by using the testing data is still achieved.

The overall results demonstrated the importance of the interpretability in data-driven AHU diagnostic strategies. Due to the inherent limitation of data-driven diagnostic strategies, AHU faults that do not have a unique data pattern or are outside the operating conditions covered in the training data are difficult to be isolated. In general, data-driven methods are superior in extracting the useful information from large data sets and modelling the behavior of HVAC systems. Expert knowledge can play a role in assisting in interpreting and validating the information and knowledge discovered by the data-driven methods. Therefore, combining

data-driven methods with expert knowledge might be a possible solution for developing effective data-driven based fault diagnostic strategies.

Acknowledgment

The authors would like to sincerely thank ASHRAE for granting the permission to use the data from ASHRAE 1312-RP to validate the strategy developed.

References

[1] V. Gunes, S. Peter, T. Givargis, Improving energy efficiency and thermal comfort of smart buildings with HVAC systems in the presence of sensor faults, in: IEEE 17th International Conference on High Performance Computing and Communications (HPCC), 2015, 2015, pp. 945–950.
[2] Z. Ma, S. Wang, Fault-tolerant supervisory control of building condenser cooling water systems for energy efficiency, HVAC&R Res. 18 (1–2) (2011) 126–146.
[3] Z. Ma, S. Wang, Online fault detection and robust control of condenser cooling water systems in building central chiller plants, Energy Build. 43 (1) (2011) 153–165.
[4] S. Katipamula, M.R. Brambley, Methods for fault detection, diagnostics, and prognostics for building systems - a review (Part I), HVAC&R Res. 11 (1) (2005) 3–25.
[5] R. Yan, Z. Ma, G. Kokogiannakis, Y. Zhao, A sensor fault detection strategy for air handling units using cluster analysis, Autom. Constr. 70 (2016) 77–88.
[6] Z. Du, B. Fan, J. Chi, X. Jin, Sensor fault detection and its efficiency analysis in air handling unit using the combined neural networks, Energy Build. 72 (2014) 157–166.
[7] H. Yang, S. Cho, C.S. Tae, M. Zaheeruddin, Sequential rule based algorithms for temperature sensor fault detection in air handling units, Energy Convers. Manage. 49 (8) (2008) 2291–2306.
[8] Y. Zhao, J. Wen, F. Xiao, X. Yang, S. Wang, Diagnostic bayesian networks for diagnosing air handling units faults – Part I: faults in dampers, fans, filters and sensors, Appl. Therm. Eng. (2016), http://dx.doi.org/10.1016/j.applthermaleng.2015.09.121, available online.
[9] Y. Zhao, J. Wen, S. Wang, Diagnostic Bayesian networks for diagnosing air handling units faults –Part II: Faults in coils and sensors, Appl. Therm. Eng. 90 (2015) 145–157.
[10] H. Wang, Y. Chen, C.W.H. Chan, J. Qin, J. Wang, Online model-based fault detection and diagnosis strategy for VAV air handling units, Energy Build. 55 (2012) 252–263.
[11] L.H. Chiang, R.D. Braatz, E.L. Russell, Fault Detection and Diagnosis in Industrial Systems, Springer London, Great Britain, 2001.
[12] S. Wang, F. Xiao, AHU sensor fault diagnosis using principal component analysis method, Energy Build. 36 (2) (2004) 147–160.
[13] Z. Du, X. Jin, L. Wu, Fault detection and diagnosis based on improved PCA with JAA method in VAV systems, Build. Environ. 42 (9) (2007) 3221–3232.
[14] Z. Du, X. Jin, Multiple faults diagnosis for sensors in air handling unit using Fisher discriminant analysis, Energy Convers. Manage. 49 (12) (2008) 3654–3665.
[15] W.Y. Lee, J.M. House, D.R. Shin, Fault diagnosis and temperature sensor recovery for an air-handling unit, Trans.-Am. Soc. Heating Refrigerating Air Conditioning Eng. 103 (1997) 621–633.
[16] J. Liang, R. Du, Model-based fault detection and diagnosis of HVAC systems using support vector machine method, Int. J. Refrig. 30 (6) (2007) 1104–1114.
[17] T. Mulumba, A. Afshari, K. Yan, W. Shen, L.K. Norford, Robust model-based fault diagnosis for air handling units, Energy Build. 86 (2015) 698–707.
[18] I.T. Jolliffe, Principal Component Analysis, Springer-Verlag, New York, 1986.
[19] M. Padilla, D. Choinière, A combined passive-active sensor fault detection and isolation approach for air handling units, Energy Build. 99 (2015) 214–219.
[20] B. Fan, Z. Du, X. Jin, X. Yang, Y. Guo, A hybrid FDD strategy for local system of AHU based on artificial neural network and wavelet analysis, Build. Environ. 45 (12) (2010) 2698–2708.
[21] Z. Du, X. Jin, Y. Yang, Fault diagnosis for temperature, flow rate and pressure sensors in VAV systems using wavelet neural network, Appl. Energ. 86 (9) (2009) 1624–1631.
[22] W.Y. Lee, J.M. House, C. Park, G.E. Kelly, Fault diagnosis of an air-handling unit using artificial neural networks, Trans.-Am. Soc. Heating Refrigerating Air Conditioning Eng. 102 (1996) 540–549.
[23] Z. Du, B. Fan, X. Jin, J. Chi, Fault detection and diagnosis for buildings and HVAC systems using combined neural networks and subtractive clustering analysis, Build. Environ. 73 (2014) 1–11.
[24] W.-Y. Lee, J.M. House, N.-H. Kyong, Subsystem level fault diagnosis of a building's air-handling unit using general regression neural networks, Appl. Energ. 77 (2) (2004) 153–170.
[25] J. Wall, Y. Guo, J. Li, S. West, A dynamic machine learning-based technique for automated fault detection in HVAC systems, ASHRAE Trans. 117 (part 2) (2011) 449–456.
[26] Z. Yu, F. Haghighat, B.C.M. Fung, H. Yoshino, A decision tree method for building energy demand modeling, Energy Build. 42 (10) (2010) 1637–1646.
[27] K. Basu, L. Hawarah, N. Arghira, H. Joumaa, S. Ploix, A prediction system for home appliance usage, Energy Build. 67 (2013) 668–679.
[28] K. Bruton, P. Raftery, B. Kennedy, M. Keane, D.T.J. O'sullivan, Review of automated fault detection and diagnostic tools in air handling units, Energy Effic. 7 (2) (2014) 335–351.
[29] S. Li, A Model-Based Fault Detection and Diagnostic Methodology for Secondary HVAC Systems, Ph.D. Thesis, College of Engineering, Drexel University, 2009.
[30] P.N. Tan, M. Steinbach, V. Kumar, Introduction to Data Mining, Pearson Addison Wesley, USA, 2006.
[31] W.Y. Loh, Classification and regression trees, Wiley Interdiscip. Rev.: Data Min. Knowl. Discov. 1 (1) (2011) 14–23.
[32] L. Rokach, Data Mining with Decision Trees: Theory and Applications, World Scientific, Singapore, 2008.
[33] Y. Yohannes, P. Webb, Classification and regression trees, in: CART: A User Manual for Identifying Indicators of Vulnerability to Famine and Chronic Food Insecurity, International Food Policy Research Institute, 1999.
[34] L. Breiman, J. Friedman, R.A. Olshen, C.J. Stone, Classification and Regression Trees, Wadsworth, Inc, USA, 1984.
[35] L.F.R.A. Torgo, Inductive Learning of Tree-based Regression Models, Ph.D Thesis, Department of Computer Science University of Porto, 1999.
[36] R. Development Core Team, R: A Language and Environment for Statistical Computing [Software], R Foundation for Statistical Computing, Vienna, Austria, 2008.
[37] T. Therneau, B. Atkinson, B. Ripley, rpart: Recursive Partitioning and Regression Trees, 2015.
[38] S. Milborrow, rpart.plot: Plot 'rpart' Models: An Enhanced Version of 'plot.rpart', (2015).
[39] H. Wickham, Ggplot2: Elegant Graphics for Data Analysis, Springer, New York, 2009.
[40] S. Li, J. Wen, Description of fault test in Summer of 2007, In: ASHRAE 1312 Report, 2007.
[41] S. Li, J. Wen, X. Zhou, C.J. Klaassen, Development and validation of a dynamic air handling unit model, Part 1, ASHRAE Trans. 116 (1) (2010) 45–56.
[42] S. Li, J. Wen, X. Zhou, C.J. Klaassen, Development and validation of a dynamic air handling unit model, part 2, ASHRAE Trans. 116 (1) (2010) 57–73.
[43] L.K. Norford, J.A. Wright, R.A. Buswell, D. Luo, C.J. Klaassen, A. Suby, Demonstration of fault detection and diagnosis methods for air-handling units, HVAC&R Res. 8 (1) (2002) 41–71.